RAINFALL ESTIMATION FROM SATELLITE IMAGES

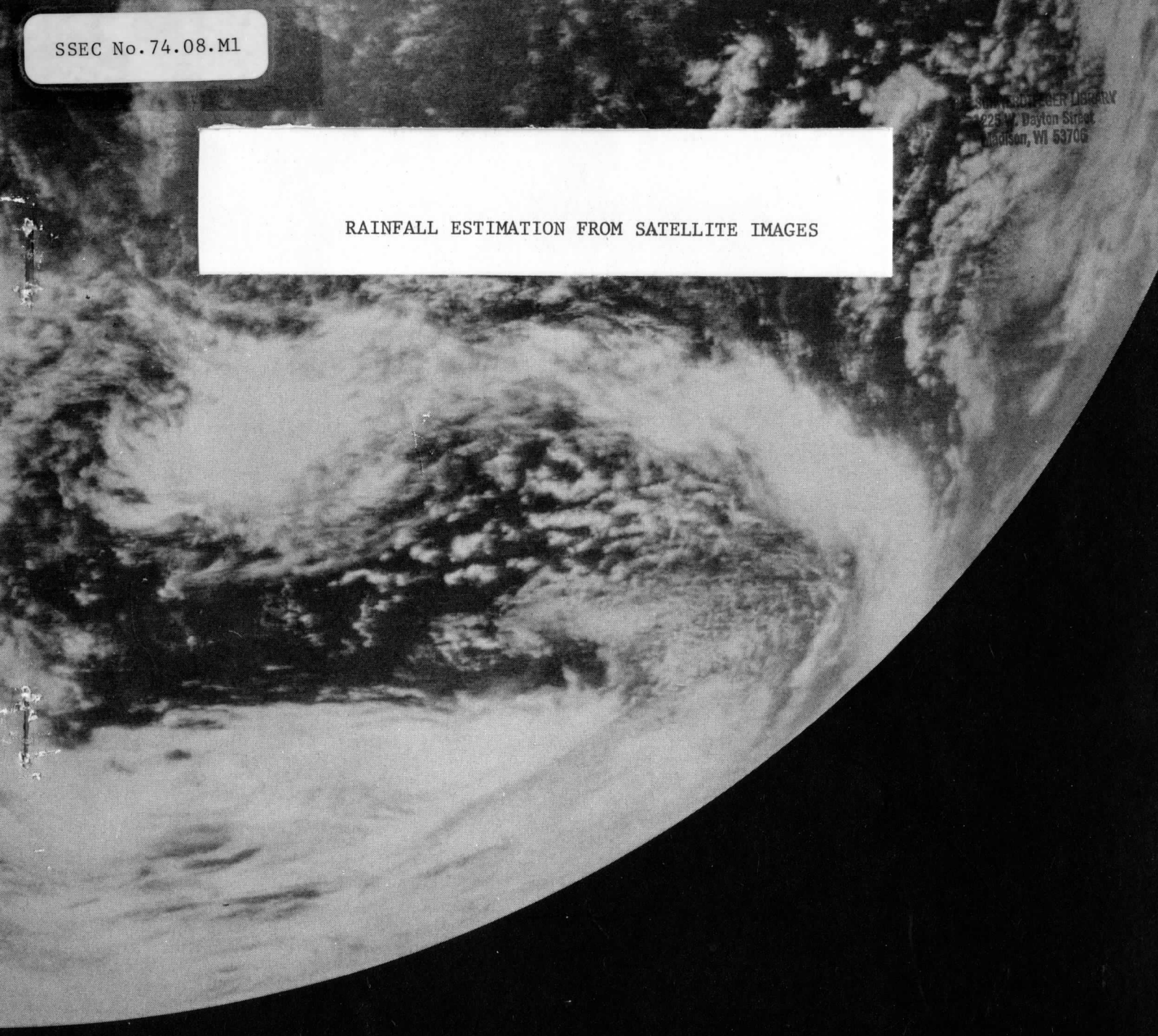

A REPORT

from the space science and engineering center
the university of wisconsin-madison
madison, wisconsin

RAINFALL ESTIMATION FROM SATELLITE IMAGES

David W. Martin
Dhirendra N. Sikdar

Space Science and Engineering Center
The University of Wisconsin
Madison

August 1974

Report on NOAA Contract 03-4-022-22

Table of Contents

ACKNOWLEDGEMENTS

John Stout and Gary Chatters contributed substantially through several stages of this program. Richard Maconi assisted in the tedious task of data analysis. Figures were very capably drafted by Dana Wooldridge. Mrs. Helen Loeb typed most of the text.

I. INTRODUCTION

This interim report covers progress and problems over the period of the second year of the SSEC-Experimental Meteorology Laboratory rainfall estimation program, begun in July 1973. It also summarizes the status of the method in respect to prospects for its successful use for GATE. A summary of the summer 1973 satellite and radar data set is followed by a description of the method now used for data processing. Discussion of the status of data processing precedes sections on results to date and a test case based on a preliminary cloud-rainfall relation. For details of earlier work, see the first year contract report, "Calibration of ATS-3 Images for Quantitative Precipitation Estimation," (July 1973). The third year proposal, "Rainfall Estimation from Satellite Images: A Proposal for GATE," (March 1974) details plans for use of the method to estimate rainfall over wave and cluster (A and B) scales following GATE.

II. DATA AND DATA PROCESSING

~~On~~ For selected days in the summer of 1973, NOAA's Experimental Meteorology Laboratory (EML) created copies of digital tapes of images from their 10-cm WSR-57 radar. The first tape sent to SSEC contained power returned, and the rest rainfall estimates.

On June 12, 1973, SSEC's J.T. Young visited the Wallops Island Ground Station in an effort to control the gain in ATS-3 pictures. The variable gain amplifier in the video processor unit was replaced by a fixed gain amplifier. A routine schedule was set up for adjusting the demux, video level, and noise level. Series of pictures covering up to a six hour period were digitized by NASA for SSEC. The interval between picture times is shorter in 1973 (20 min.) than in 1972 (28 min.).

Gain levels are tested by a calibration technique developed at SSEC by Fred Mosher. An infinitely deep and wide cloud is assumed to exist in every day sequence, and have the same reflective characteristics. A standard brightness for the same sun and satellite geometry is calculated using a multiple-scattering method (Mosher, NASA Final Report, 1973). The ratio (α) of this standard brightness over the observed brightness provides a means to compare and equivalence picture series on different days.

A graph of alpha values and the decibel change from alpha = 1 is shown in Figure 1. A documented 2 db change on August 1, 1972 (day 214) was accurately predicted by calibrations on days 195 and 230. This gave early confidence in both the calibration and the documentation of gain changes. Later calibrations proved troublesome. For example, a 3.6 db gain change between days 230 and 346 would be expected from the calibrations, yet no change was documented.

Close examination of some 1973 clouds used for calibration revealed a phenomenon we have named the "bright line problem." In the very bright clouds used for calibration, some lines at regular intervals (e.g. 9 lines) were consistently brighter than their fellows only for the length of the cloud itself. This has been found in all our 1973 data, which comes through the Westinghouse system, as well as in 1974 real time data coming through the Hughes system. An example is shown in Figure 2.

For purposes of calibration, we have made calculations of alpha with bright lines removed. But this is subjective, and one does not know if there are "somewhat bright lines" too. It is suggested, however, by frequency distribution plots of ocean surface brightness, that for our 1972 and 1973 data sets gain levels between documented changes remained relatively stable.

B. Data Processing

There have been substantial improvements in the method of generating sta-

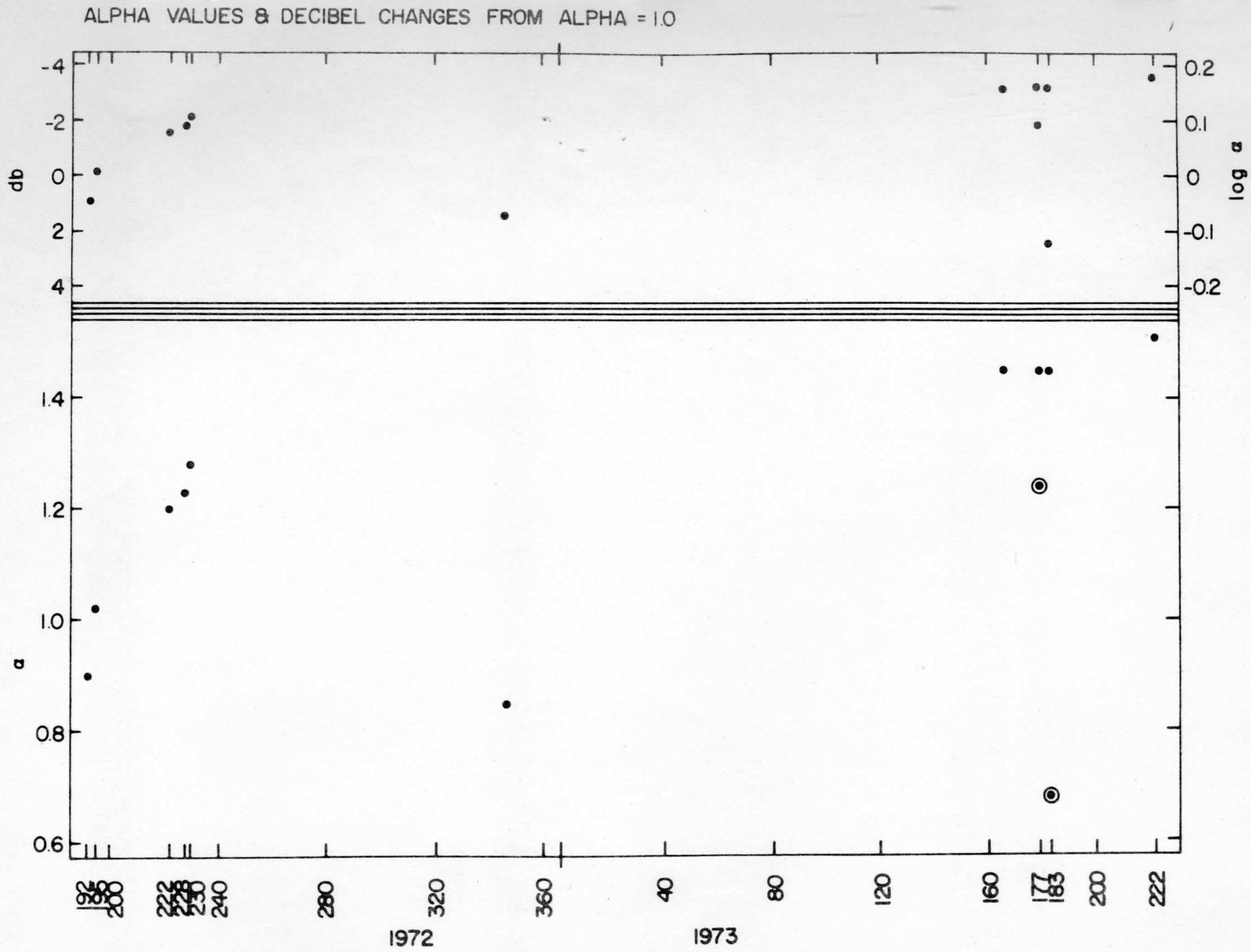

Figure 1. Alpha (standard brightness/brightness recorded by satellite) and decibel changes [20 $\log_{10}(\alpha_1/\alpha_2)$] from $\alpha_1 = 1.0$.

The circled points are those uncorrected for bright lines.

BRIGHT LINE 25°N 92°W
DAY 183/73

1716z

Figure 2. Three bright lines, 17 lines apart

tistics for use in developing a rainfall estimation technique. A general summary precedes discussion of improvements.

ATS-3 and radar images are displayed on a TV monitor. Cloud outlines are drawn and given numbers. Echoes are matched with individual clouds. Cloud and echo area and cloud maximum brightness are recorded. (Cloud area is defined as the number of pixels brighter than a threshold value times area per pixel.) Echo area through the Florida z-r relationship gives an estimate of rainfall. Cloud area and maximum brightness as a function of time are then compared to the associated echo area or rainfall estimate as a function of time.

Figure 3 outlines the old and new data processing steps. In the section labeled Preprocessing-Radar, one computer run replaces many steps formerly done by hand. Previously, transferring from source to microfilm to positive print to digital tape resulted in considerable smudging of information and introduction of other sources of error. Echo information now is transferred directly from source to digital tape (Wiggert and Andrews, 1974 and Wiggert and Östlund, 1974).

The most significant improvement in Preprocessing-ATS is normalization. The effect of changing sun and satellite angle is eliminated by normalizing to a standard sun and satellite geometry, in our case, noon of July 1, 1972 at Miami. Normalization is accomplished through the same multi-scattering technique used in calibration. Another difference is the shifting of the ATS image itself to match the echo pattern rather than the shifting of the acetate with the cloud outlines. This gives an extremely accurate local navigation, and permits the direct comparison of radar and ATS images.

As in Preprocessing-Radar, many processing steps have been consolidated and made more accurate through the use of McIDAS. Whereas previously the taking of statistics on a cloud involved a dozen or more hand copying steps, it now

DATA PROCESSING

PREPROCESSING

OLD

ATS	RADAR
Digitize from analog (if digital tapes not available)	Select microfilm to match ATS time
quality control	print photo of radar image
navigate	point out range lines, clutter
remap	digitize from painted photo
load	navigate
	remap
	load

NEW

ATS	RADAR
quality control copy to 9 track from archive	remap
navigate	
calibrate	
navigate cloud field on echo pattern	
normalization	
make radar - ATS save tapes	

PROCESSING

OLD

Outline and label clouds and echoes on acetate

Match cloud and echo pattern

Write down coordinates of boxes

Transform TV→ tape coordinates on a hand calculator

Keypunch a card for each box

Carry tapes and deck to 1110 to run statistics program that outputs cumulative histograms

Extract statistics from histograms

NEW

Outline and label clouds on acetate

Take statistics (square box or hand drawn outline)

Take picture of image with outline and label overlayed

Figure 3. DATA PROCESSING

is simply a matter of tracing the cloud outline and pressing a few keys. Location, maximum brightness, and areas within 8 contour brightness levels almost instantly appear. The computer stores the outline and later overlays it and those of other clouds for documentation in the form of a photograph, as in Figure 4. It is also far more accurate to trace a cloud's irregular outline than to approximate the same by up to 4 rectangles. Finally, instant black and white and color enhancement allows more precise location of cloud borders.

There has also been a change in the way clouds are defined. Our original approach was to consider each brightness maximum is a cloud. Objective cloud discrimination and the splitting and merging of clouds caused many headaches. In the new approach, which was used on the best 4 days in 1972, a larger scale is considered, with clouds separated by a definite darker area. Another aspect of this new approach is to start the labeling and drawing of cloud outlines at the time when the organization is clearest, instead of at the beginning. This will usually be near or at the end of a sequence, since over Florida, circulation patterns typically become stronger as systems mature in the afternoon. An attempt is also made to look at the entire sequence, following individual clouds. This eliminates most of the surprises and relabeling and outline-drawing, and results in a division into clouds more consistent with the behavior throughout the sequence. We also ignore small short-lived clouds, which contribute a very small amount to the total precipitation.

C. Status

The four best day series of 1972 were re-done by the Reverse Sequence Method described above. All the changes outlined in section IIB were implemented in processing four days in 1973. EML is processing radar images for two of these days. The ATS images for those two and both the ATS and radar images for the other two days have been processed on McIDAS. Processing on one more day

Figure 4. Clouds with outlines and cloud numbers overlaid. The 1934Z, 1953Z and 2012Z pictures have been normalized.

is planned. Since in each of the sequences so far processed there is an average of 10 to 15 distinct clouds and cloud systems, these five days should yield a sample large enough to bear detailed statistical analysis.

III. RESULTS

An example of 1972 data re-done with the Reverse Sequence Method is shown in Figure 5. This graph of cloud and echo area versus time illustrates two problems with the 1972 data set. Neither the cloud area nor echo area maximum has been reached by the end of the sequence and we are seeing only part of the growing stage of the cloud. Longer sequences in 1973 days have eliminated most of this problem for that year. The other problem is a certain bumpiness, especially apparent in the cloud area data. This is probably due to approximating the cloud's outline by rectangles. In processing the 1973 data, the cloud's boundary was directly traced with McIDAS. Even with these problems, an average of 1972 data showed echo area peaking about one hour before the maximum in cloud area (see Figure 6).

Day 222 is the first from 1973 to be completed. The quality of the results is clearly superior to the 1972 data set. Figures 7 and 8 present evolutions of two clouds, a high brightness cloud (cumulonimbus), and a low brightness cloud (probably congestus). In the first, a peak in rainfall precedes a flatter peak in cloud area by an hour and 45 minutes. The small cloud exhibits a complex evolutionary cycle. Two maxima are separated by 3 hours and 15 minutes with only one having a clear association with rain.

The cloud-rain relationship is being formulated as a Woodley diagram in which volumetric rainfall(V_R) and cloud area (A) are normalized by dividing by maximum cloud area (A_{mx}). Events before the time of maximum cloud area are placed to the left of the center, those after to the right. For day 222, clouds have been divided into two classes, those with maximum brightness greater

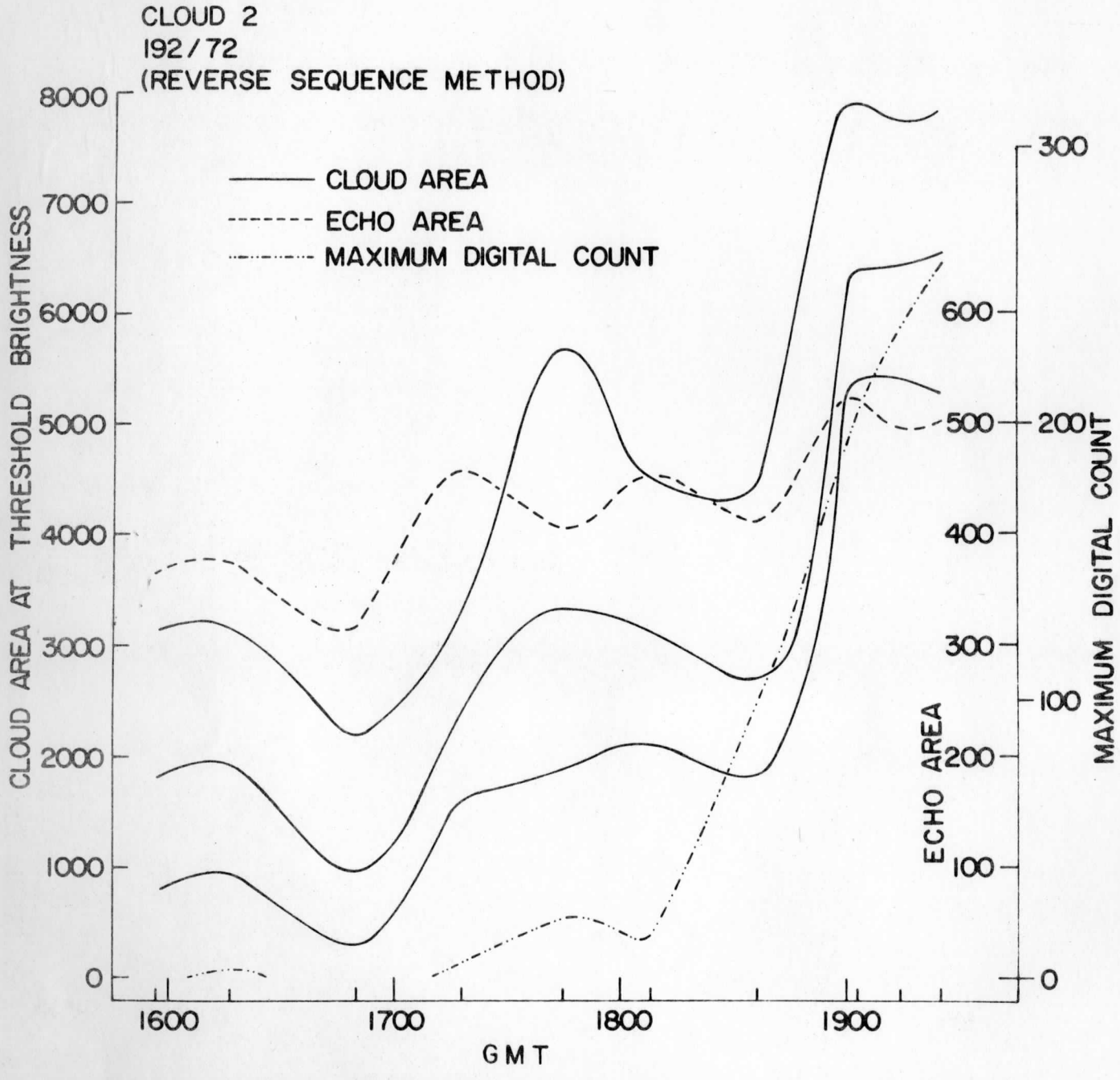
CLOUD 2
192/72
(REVERSE SEQUENCE METHOD)
CLOUD AREA
ECHO AREA
MAXIMUM DIGITAL COUNT
CLOUD AREA AT THRESHOLD BRIGHTNESS
8000
7000
6000
5000
4000
3000
2000
1000
0
ECHO AREA
300
600
500
400
300
200
100
MAXIMUM DIGITAL COUNT
1600
1700
1800
1900
GMT

Figure 5

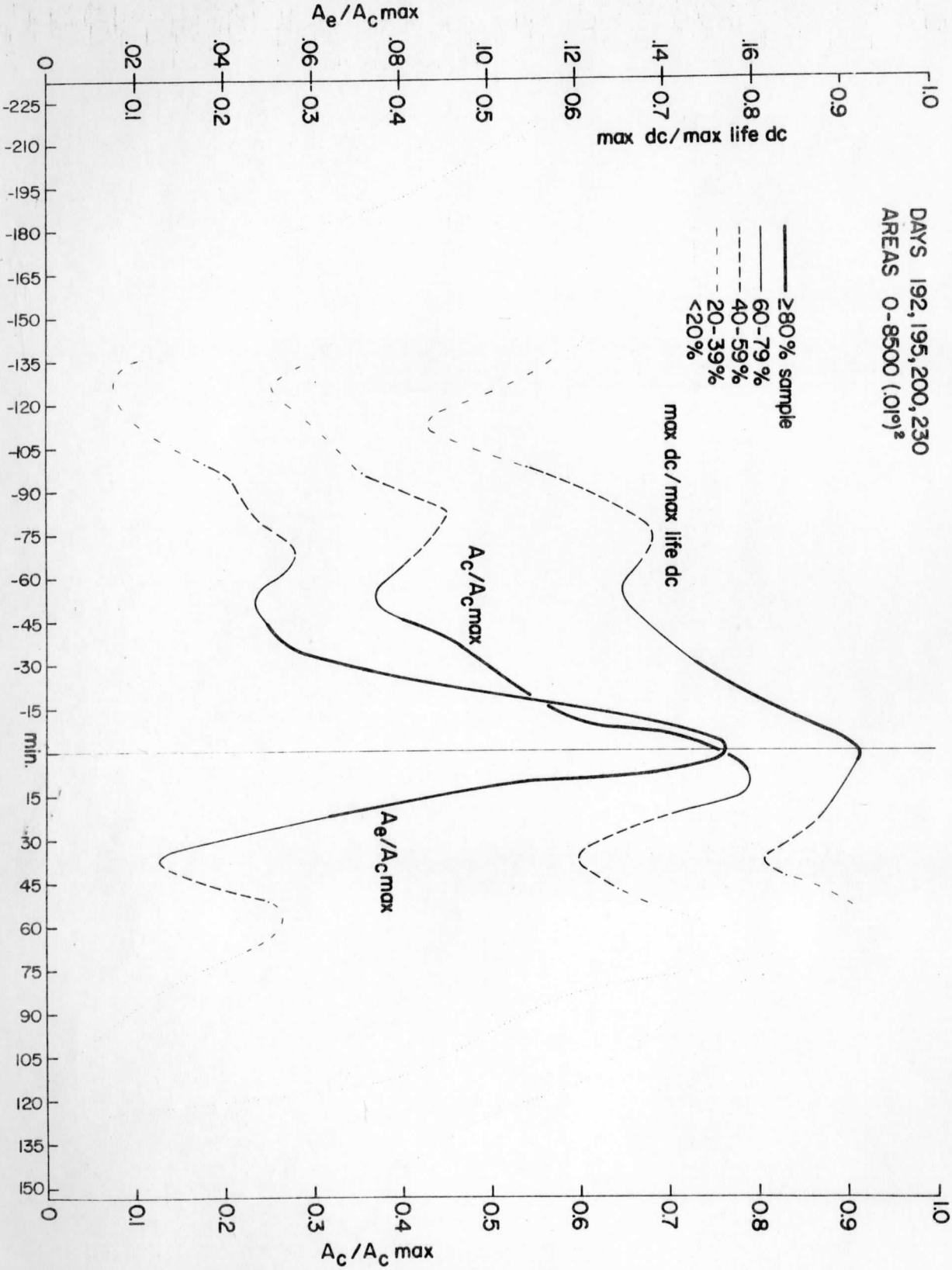

Figure 6. Time averaged, size normalized cloud area (A_c/A_c max) and echo area (A_e/A_c max), and maximum brightness or digital count (max dc/ max life dc) for 1972 clouds processed with the Reverse Sequence Method. A_c max and max life dc are the greatest cloud area and greatest maximum brightness over the lifetime of the cloud. The time of maximum echo area is taken as time zero. The fraction of the total number of clouds present at a given time is denoted as % sample.

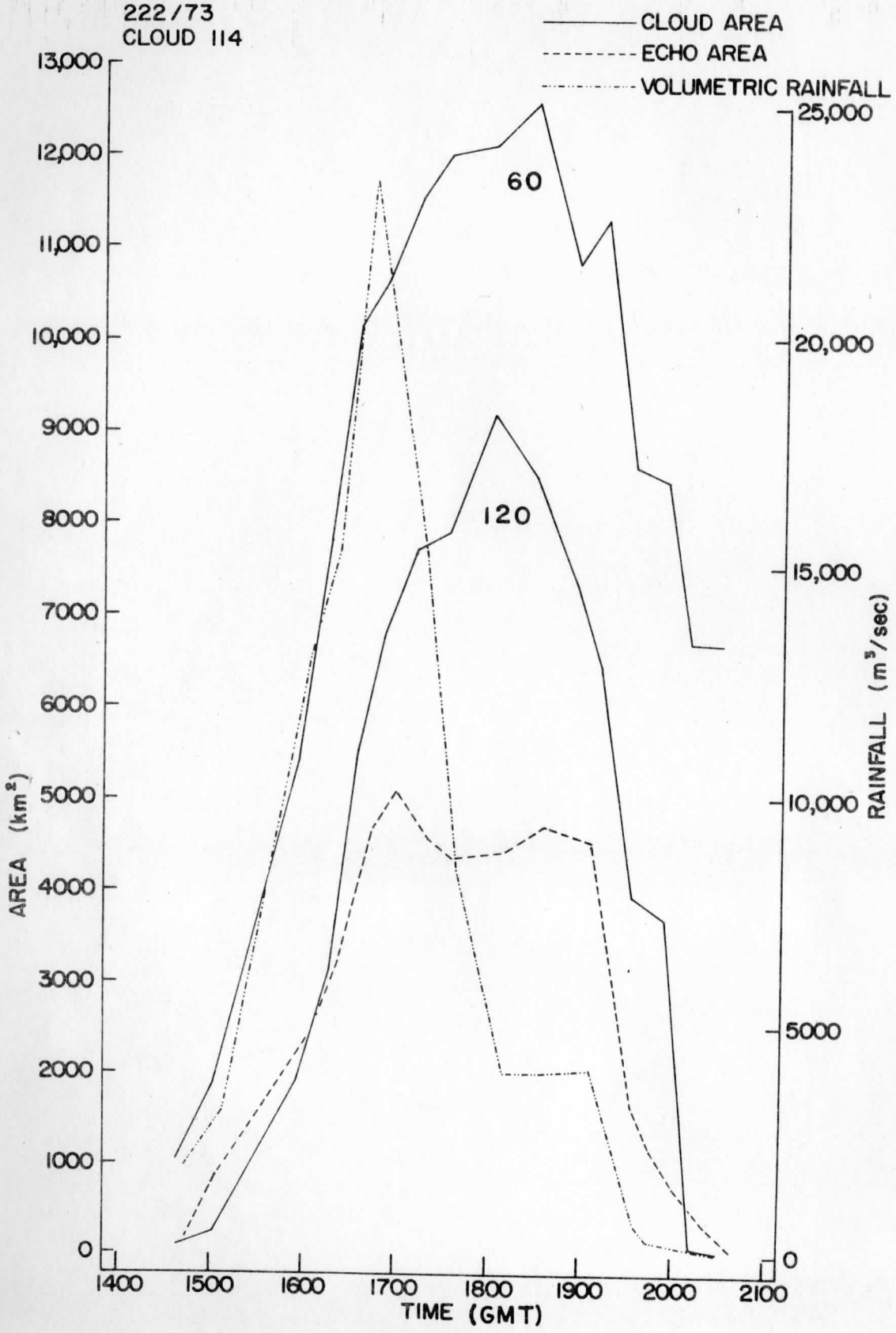

Figure 7. Cloud area defined at 60 and 120 digital brightness contour levels and rainfall vs. time for a high brightness cloud.

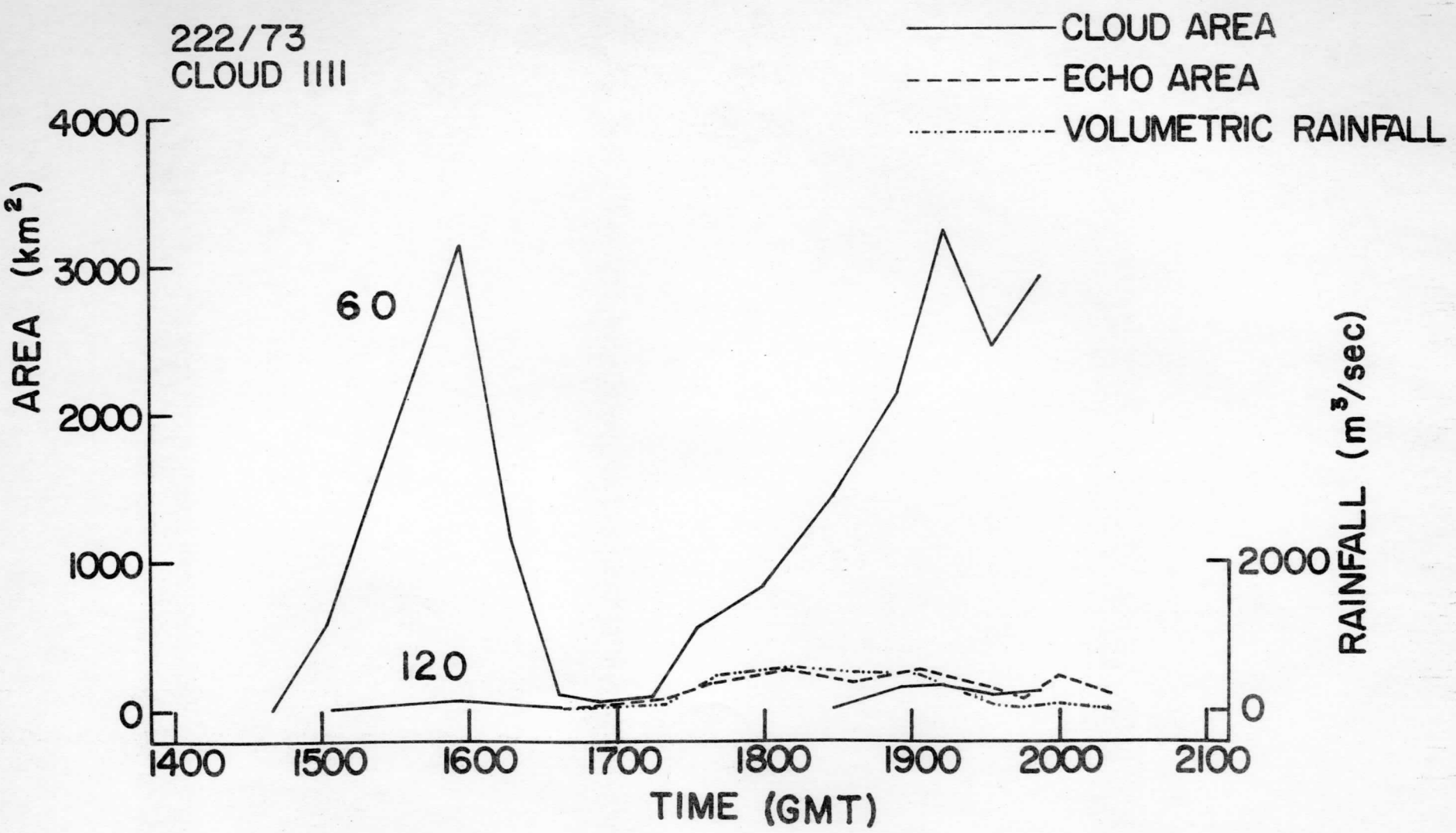

Figure 8. Cloud area defined at 60 and 120 digital brightness contour levels and rainfall vs. time for a low brightness cloud.

than 160 digital counts, and less than 150 digital counts. The individual diagrams from each class is shown in Figures 9 and 10, and averaged diagrams for each class in Figure 11. As in the cloud area-rainfall graphs (Figures 7 and 8), the brighter clouds exhibit a sharp, well-defined rain peak before the cloud maximum and the dimmer clouds show confused and flat behavior. Clouds undergoing more than one evolutionary cycle present a loop in Figures 9 and 10. Rainfall estimation is easy. Given a cloud area and the knowledge of which side of A_{mx} it is on, V_R/A_{mx} can be read off the ordinate. Multiplying by maximum cloud area gives the volumetric rainfall rate.

A matrix of correlation coefficients between volumetric rainfall and cloud area of day 222 is presented in Figure 12. The axes are the different brightness levels used to define cloud area, and the time lags. A lag of positive one occurs when the correlation is between cloud areas at time t and rainfall at time t-20 minutes. The correlation peak at a lag of one hour is in agreement with the rainfall-cloud area lag seen in Figure 7. The symmetrical dropoff from the peak in the lag direction means that the cloud area curves are symmetrical in time. Near the one hour lag peak the areas defined by higher brightness levels give better correlations than lower levels; away from this peak they do not. This suggests that when present, the former are a better indicator of precipitation.

Clouds on day 222 were stratified into categories of land, sea, and both. However, the landward movement of the majority meant that most fell into the "both" category. Those which did not form a sample too small to draw conclusions from; thus evaluation of land-sea differences must await a larger sample.

IV. TESTING

A test using the Woodley diagram was made on an isolated rapidly growing cloud cluster in the tropical Atlantic on day 203 (22 July 1969). The cluster's

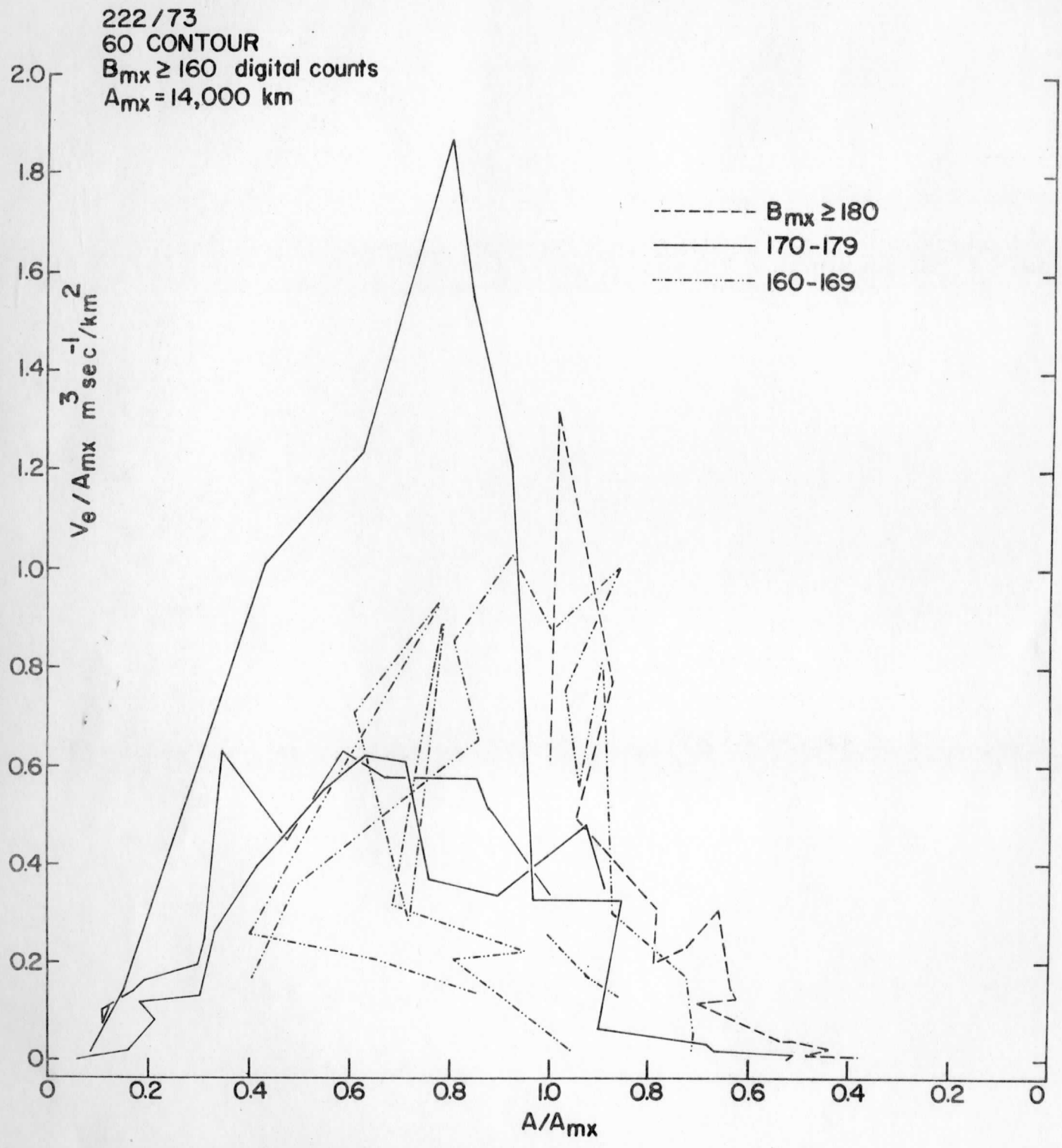

Figure 9. Woodley diagrams for clouds with maximum digital count greater than or equal to 160. The average A_{mx} is 14,000 square km.

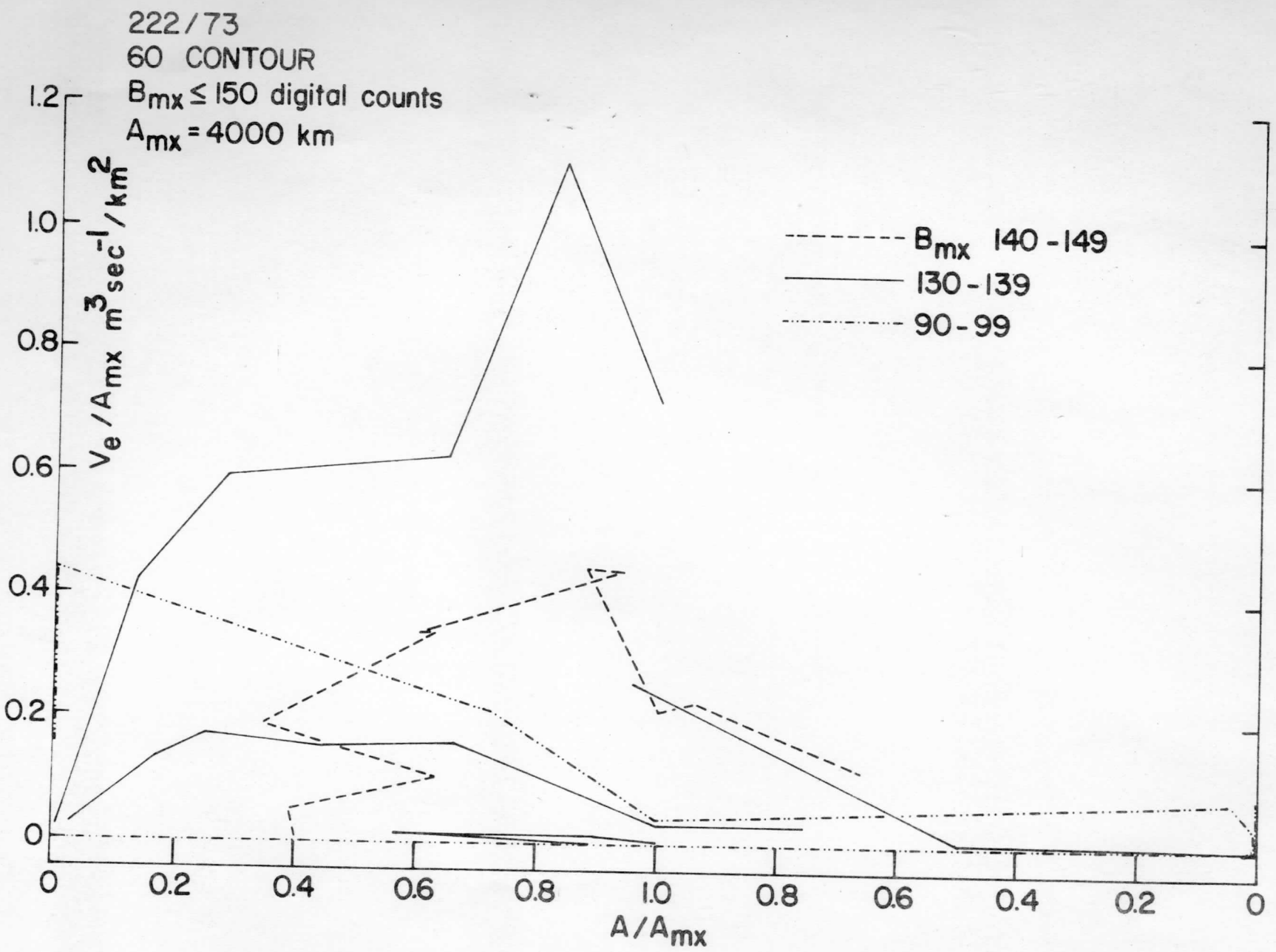

Figure 10. Woodley diagrams for clouds with maximum digital count less than or equal to 150. The average A_{mx} is 4,000 square km.

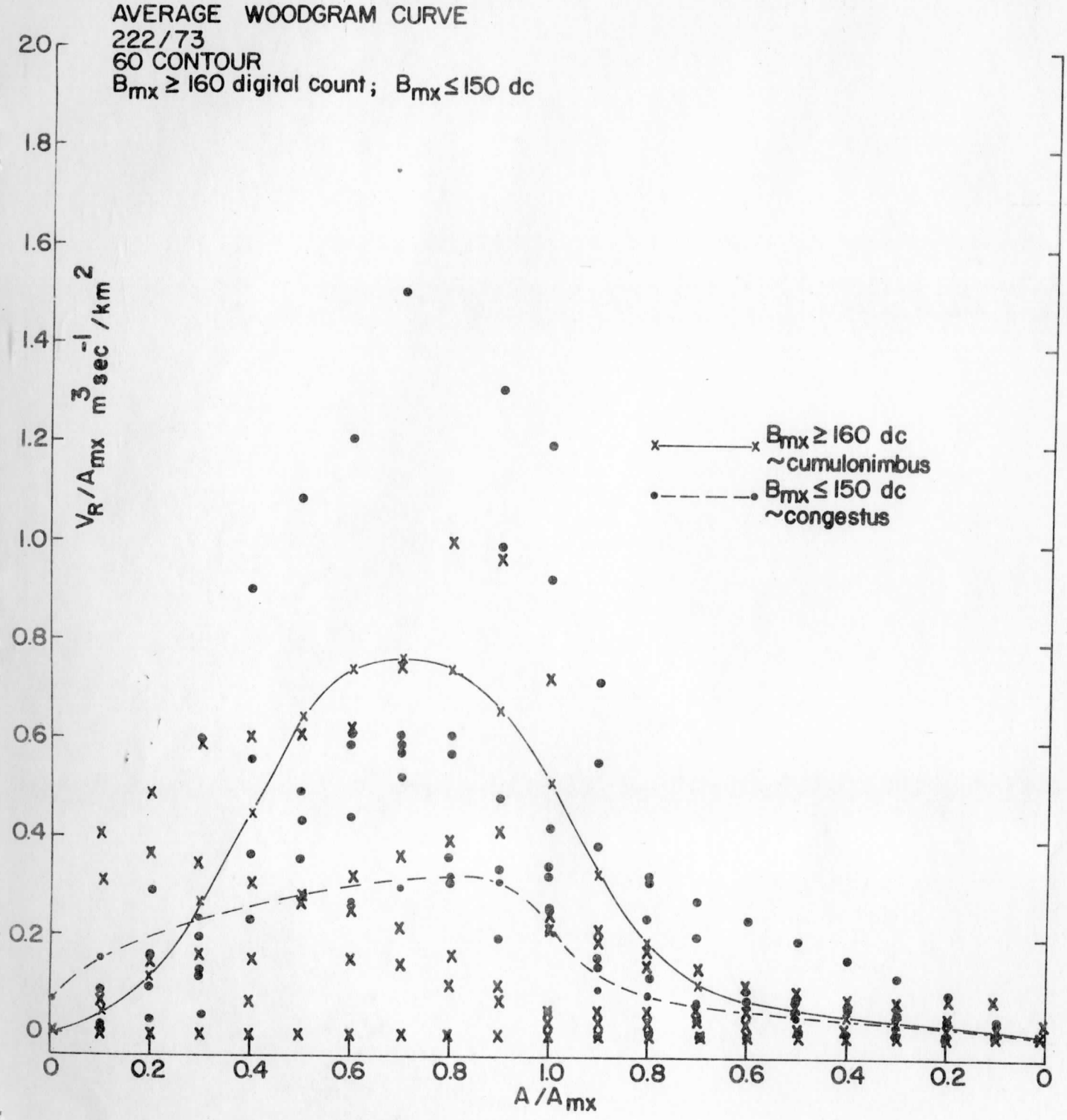

Figure 11. Average Woodley diagrams for maximum digital count greater than or equal to 160, and less than or equal to 150.

DAY 222

LEVEL / LAG	40	50	60	70	80	90	105	120
-3	.5339	.5126	.4965	.4831	.4682	.4649	.4412	.4442
-2	.6355	.6201	.6064	.5935	.5798	.5789	.5626	.5690
-1	.7101	.7028	.6982	.6863	.6746	.6752	.6692	.6793
0	.7667	.7606	.7560	.7457	.7397	.7419	.7528	.7691
1	.7962	.7953	.7942	.7865	.7847	.7877	.8064	.8290
2	.8145	.8193	.8213	.8177	.8193	.8267	.8485	.8785
3	.8243	.8342	.8390	.8416	.8452	.8575	.8796	.9133
4	.8185	.8321	.8391	.8494	.8547	.8728	.8939	.9223
5	.7899	.8040	.8103	.8240	.8322	.8566	.8792	.8925
6	.7645	.7783	.7854	.8023	.8114	.8381	.8535	.8352
7	.7240	.7370	.7437	.7604	.7717	.7951	.7980	.7358

1 LAG = 20 min.

Figure 12. Correlation coefficients between cloud area and volumetric rainfall at different levels used to define cloud area, and different time lags.

dynamic and thermodynamic environment has been studied by Martin and Sikdar (1974). Evolutionary changes in different parts of the cloud ensemble are presented in Figure 13. Figure 14 is the rainfall estimate, made from the cloud area-rain volume curves shown in Figure 11. Precipitation for the whole cloud cluster varied between 3 and 6 x 10^3 m^3/sec.

This cloud area estimate of total rainfall from the cluster was compared with an independent moisture budget rain estimate. In a separate program (Suomi, Sikdar and Martin, 1974), the horizontal mass convergence for this cluster has been derived for the period 1545-1638Z from cloud motion vectors, and vertical mass flux through the equation of continuity. With an average mixing ratio 18 gm/Kg and estimated mass flux 13.4 x 10^8 Kg/sec, the water vapor transport through the lifting condensation level amounted to 2.4 x 10^{10} gm/sec, on the cluster scale. Assuming that 50% of this condensed water rained out, the precipitation rate becomes 12 x 10^3 m^3/sec, about two times the rate derived from the brightness technique for that time period. The difference, given uncertainties in both estimates, is sufficiently small to encourage an optimism that with the superior data of SMS, this technique is adequate to the task of providing scientifically useful rainfall estimates for GATE.

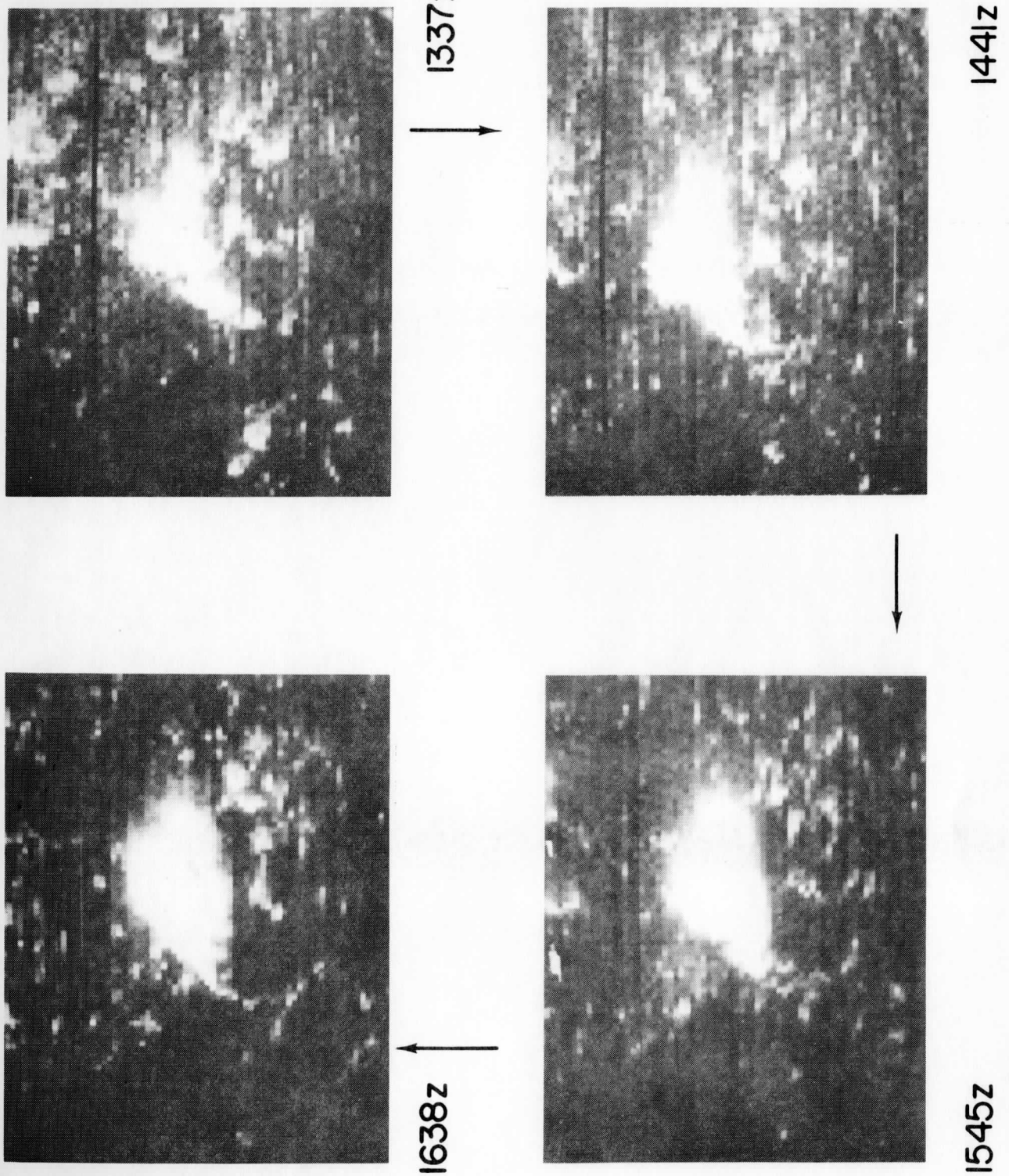

Figure 13. Cloud evolution in test case.

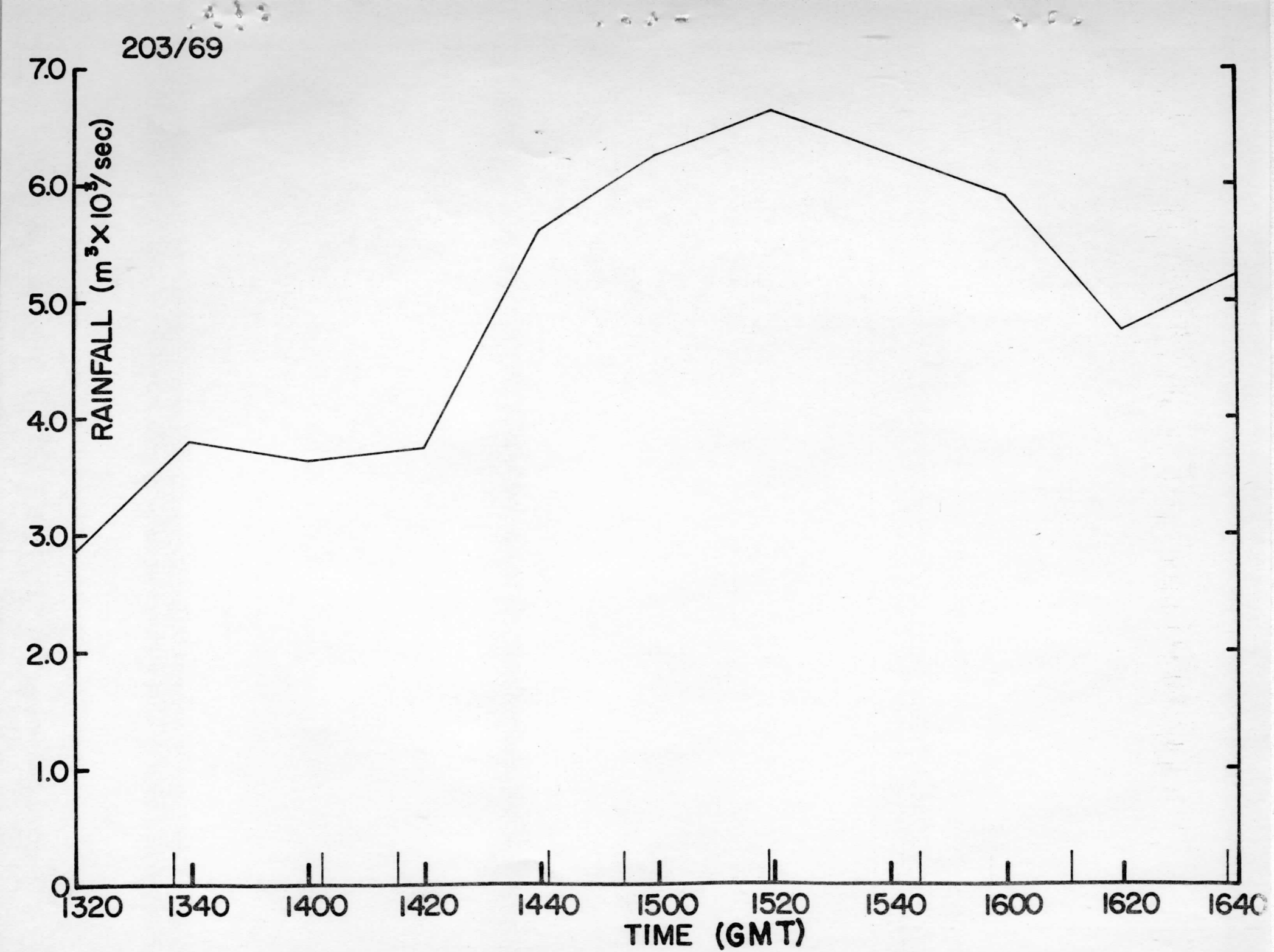

Figure 14. Precipitation estimation by Woodley diagram for test case.

REFERENCES

Martin, David W., and Dhirendra N. Sikdar, July 1973: Calibration of ATS-3 Images for Quantitative Precipitation Estimation.

Martin, David W., Dhirendra N. Sikdar, and Verner E. Suomi, March 1974: Rainfall Estimation from Satellite Images: A Proposal for GATE.

Mosher, Frederick R., 1973: Cloud Brightness Contrast as Viewed by a Satellite, Measurements from Satellite Systems, Annual Scientific Report on NAS 5-21798.

Wiggert, B., and G. S. Andrews, May 1974: Digitizing, Recording, and Computer Processing Weather Radar Data at the Experimental Meteorology Laboratory, NOAA Technical Memorandum, ERL WMPO-17.

Wiggert, B., and S. Östlund, 1974: "Computerized Rain Assessment and Tracking of South Florida WSR-57 Weather Radar Echoes", Bulletin of the American Meteorological Society.